International Journal of Mechanical and Production Engineering Research and Development (IJMPERD)
ISSN(P): 2249–6890; ISSN(E): 2249–8001
Vol. 9, Issue 5, Oct 2019, 1179–1190

TRANS STELLAR
•Journal Publications •Research Consultancy

MIXED CONVECTIVE HEAT TRANSFER IN A RECTANGULAR NANOFLUID FILLED CAVITY WITH INCLINED MAGNETIC FIELD

S. MUTHUKUMAR[1], ESWARI PREM[2] & S. SURESH KUMAR[3,*]

[1]*Department of Mathematics, K. S. Rangasamy College of Technology, Tiruchengode, Tamil Nadu, India*

[1,2]*P. G. and Research Department of Mathematics, Government Arts College for Men, Krishnagiri, Tamil Nadu, India*

[3]*Department of Mathematics, Kongu Engineering College, Perundurai, Tamil Nadu, India*

ABSTRACT

The objective of this analysis is to discuss the effects of magnetic field and its tilted angles in a rectangular porous enclosure filled with nano fluid. The temperature at moving top wall is hot and the bottom wall remains with cold temperature, whereas the other sidewalls are adiabatic. The equations governing the considered system are solved by the finite volume method. The obtained results are discussed graphically by using isotherms, streamlines and average Nusselt number. It shows that the heat transfer rate is improved by the inclination of applied magnetic field. In the shallow cavity, the impact of Hartmann number is significant. The average Nusselt number is nearly identical when increasing Hartmann number in the slender cavity. Regardless of the permeability and the aspect ratio, enrichment in the fraction of solid and volume of nano fluid raises the overall heat transfer rate in the occurrence of magnetic field.

KEYWORDS: Magneto Hydrodynamics, Nano Fluid, Porous Medium, Aspect Ratio & Lid-Driven Cavity

Received: Jun 22, 2019; **Accepted:** Jul 12, 2019; **Published:** Oct 04, 2019; **Paper Id.:** IJMPERDOCT2019104

Original Article

1. INTRODUCTION

Fluid flow and heat transfer analysis of nanofluid in a porous enclosure, is one of the most extensively discussed problems for the last few years, owing to its uses in numerous engineering applications. Several researchers considered the shape of the cavity is square only. Many numerical simulations on convection of nanofluid in porous square cavity have been discussed by Bourantas etal. [1], Mittal et al. [2], Balla chandra shekar and Naikoti kishan [3], Kefayati [4], Hashemi et al. [5], Ghalambz et al. [6] and Astanina et al.[7]. An analysis about the properties of electrically conducting fluid influenced by the electromagnetic field is called Magneto-hydrodynamics (MHD). Several engineering and physical applications are interconnected with the MHD convection. The orientations of applied magnetic field play a key role in convectional heat transfer analysis. The impact of magnetic field in an enclosure filled with fluid or nanofluid or fluid saturated porous medium has been analyzed by Chamka [8], Malleswaran etal. [9], Muthtamilselvan and Doh [10], Elshehabey and Ahmed [11], Hussain [12], Wang etal. [13] and Grosan etal. [14]. Sometimes, the only square cavity is inadequate for such heating process, so the different shapes of cavities are required. For that, two different types of rectangular cavity are considered in this problem. This discussion examine the effects of Hartmann number, solid volume fraction and the directions of applied magnetic field in rectangular nanofluid saturated porous cavity. Following the above assessed literature review and to the author's acquaintance, so far no such discussion was carried out.

2. MATHEMATICAL MODELLING

Figure 1 represents the physical structure of the present analysis with the coordinate system. The temperature at the top wall is θ_h while at the bottom wall is θ_c such that $\theta_h > \theta_c$. Adiabatic walls are assumed at the remaining sides. The top wall is set to move in the –y direction with uniform velocity $-U_0$. It is assumed that the flow is steady, Newtonian, incompressible and laminar. The enclosure is filled with water-Cu nanofluid. According to Boussinesq approximation, the thermal properties of the nanofluid are steady excluding the density, which are given in Table 1. A uniform magnetic field B_0 is imposed perpendicular to the adiabatic sidewalls and its tilting angle is γ. Further, the viscous dissipation, induced magnetic field effect and internal heat generation are taken to be insignificant. The governing equations with boundary conditions for the considered system are as follows [2], [15]:

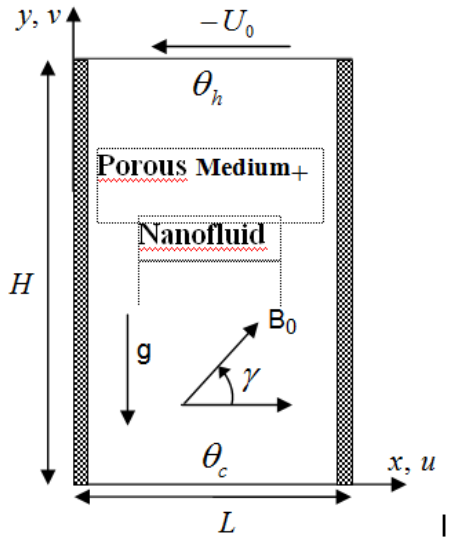

Figure 1: Physical Diagram of the Considered Study.

Table 1: Properties of Nanofluid [1], [5]

	$\rho\ (kgm^{-3})$	$C_p\ (Jkg^{-}K^{-1})$	$k\ (Wm^{-1}K^{-1})$	$\beta \times 10^{-5}\ (K^{-1})$
Base fluid (Water)	997.1	4179	0.613	21
Nanoparticles (Cu)	8933	385	401	1.67

$$\frac{\partial u}{\partial x}+\frac{\partial v}{\partial y}=0 \tag{1}$$

$$\frac{1}{\varepsilon}\left(u\frac{\partial u}{\partial x}+v\frac{\partial u}{\partial y}\right)=-\frac{\varepsilon}{\rho_{nf}}\frac{\partial p}{\partial x}+\frac{\mu_{nf}}{\rho_{nf}}\left(\frac{\partial^2 u}{\partial x^2}+\frac{\partial^2 u}{\partial y^2}\right)-\frac{\mu_{nf}}{\rho_{nf}}\frac{\varepsilon}{K}u - \frac{F\ \varepsilon}{K^{\frac{1}{2}}}u\sqrt{u^2+v^2}+\frac{\sigma_{nf}}{\rho_{nf}}\varepsilon B_0{}^2\left(v\sin\gamma\cos\gamma-u\sin^2\gamma\right) \tag{2}$$

$$\frac{1}{\varepsilon}\left(u\frac{\partial v}{\partial x}+v\frac{\partial v}{\partial y}\right)=-\frac{\varepsilon}{\rho_{nf}}\frac{\partial p}{\partial y}+\frac{\mu_{nf}}{\rho_{nf}}\left(\frac{\partial^2 v}{\partial x^2}+\frac{\partial^2 v}{\partial y^2}\right)-\frac{\mu_{nf}}{\rho_{nf}}\frac{\varepsilon}{K}v-\frac{F\ \varepsilon}{K^{\frac{1}{2}}}v\sqrt{u^2+v^2} + \frac{(\rho\beta)_{nf}}{\rho_{nf}}\varepsilon g(\theta-\theta_c)+\frac{\sigma_{nf}}{\rho_{nf}}\varepsilon B_0{}^2\left(u\sin\gamma\cos\gamma-v\cos^2\gamma\right) \tag{3}$$

$$\left(u\frac{\partial\theta}{\partial x}+v\frac{\partial\theta}{\partial y}\right)=\alpha_{nf}\left(\frac{\partial^2\theta}{\partial x^2}+\frac{\partial^2\theta}{\partial y^2}\right) \tag{4}$$

$$u=v=0,\ \theta=\theta_c,\ y=0,$$

$$u=-U_0,\ v=0,\ \theta=\theta_h,\ y=H,$$

$$u=v=0,\ \frac{\partial\theta}{\partial x}=0,\ x=0,L$$

Where, K is the permeability of the porous medium, g is the gravitational acceleration, p is the pressure, ε is the porosity and C_p is the specific heat. The K and Forchheimer's coefficient F are as follows

$$K=\frac{\varepsilon^2 d_p^2}{150(1-\varepsilon)^2},\ F=\frac{1.75}{\sqrt{150}\varepsilon^{\frac{3}{2}}}$$

Where d_p is the average particle size of the bed. The non-dimensional parameters are applied in the equations (1)–(4) are:

$$X,Y=\frac{x,y}{H},\ U,V=\frac{u,v}{U_0},\ T=\frac{\theta-\theta_c}{\theta_h-\theta_c},\ P=\frac{p}{\rho U_0^2},\ Da=\frac{K}{L^2},$$

$$Ha^2=\frac{\sigma_f B_0^2 H^2}{\mu_f},\ Gr=\frac{g\beta\Delta\theta H^3}{\nu_f^2},\ \mathrm{Re}=\frac{U_0 H}{\nu_f},\ \mathrm{Pr}=\frac{\nu_f}{\alpha_f},\ Ri=\frac{Gr}{\mathrm{Re}^2}$$

Thus, (1)–(4) becomes:

$$\frac{\partial U}{\partial X}+\frac{\partial V}{\partial Y}=0 \tag{5}$$

$$\frac{1}{\varepsilon^2}\left(U\frac{\partial U}{\partial X}+V\frac{\partial U}{\partial Y}\right)=-\frac{\rho_f}{\rho_{nf}}\frac{\partial P}{\partial X}+\frac{1}{\varepsilon}\frac{\mu_{nf}}{\rho_{nf}\nu_f\,\mathrm{Re}}\left(\frac{\partial^2 U}{\partial X^2}+\frac{\partial^2 U}{\partial Y^2}\right)-\frac{\mu_{nf}}{\rho_{nf}\nu_f}\frac{U}{Da\,\mathrm{Re}}$$
$$-\frac{1.75}{\sqrt{150}}\frac{U}{\sqrt{Da}}\frac{\left(U^2+V^2\right)^{\frac{1}{2}}}{\varepsilon^{\frac{3}{2}}}+\frac{\rho_f}{\rho_{nf}}\frac{\sigma_{nf}}{\sigma_f}\frac{Ha^2}{\mathrm{Re}}(V\sin\gamma\cos\gamma-U\sin^2\gamma) \tag{6}$$

$$\frac{1}{\varepsilon^2}\left(U\frac{\partial V}{\partial X}+V\frac{\partial V}{\partial Y}\right)=-\frac{\rho_f}{\rho_{nf}}\frac{\partial P}{\partial Y}+\frac{1}{\varepsilon}\frac{\mu_{nf}}{\rho_{nf}\nu_f\,\mathrm{Re}}-\frac{\mu_{nf}}{\rho_{nf}\nu_f}\frac{V}{Da\,\mathrm{Re}}-\frac{1.75}{\sqrt{150}}\frac{V}{\sqrt{Da}}\frac{\left(U^2+V^2\right)^{\frac{1}{2}}}{\varepsilon^{\frac{3}{2}}}$$
$$+\frac{(\rho\beta)_{nf}}{\rho_{nf}\beta_f}Ri\,T+\frac{\rho_f}{\rho_{nf}}\frac{\sigma_{nf}}{\sigma_f}\frac{Ha^2}{\mathrm{Re}}(U\sin\gamma\cos\gamma-V\cos^2\gamma) \tag{7}$$

$$\left(U\frac{\partial T}{\partial X}+V\frac{\partial T}{\partial Y}\right)=\frac{\alpha_{nf}}{\alpha_f}\frac{1}{\mathrm{Re}\,\mathrm{Pr}}\left(\frac{\partial^2 T}{\partial X^2}+\frac{\partial^2 T}{\partial Y^2}\right) \tag{8}$$

with the boundary conditions:

$$U = V = 0, \frac{\partial T}{\partial X} = 0, \; X = 0, Ar.$$

$$U = V = 0, T = 0, Y = 0,$$

$$U = -1, \; V = 0, \; T = 1, Y = Ar,$$

Where Re, Gr, Ri, Ha, Pr and Da stand for Reynolds, Grashof, Richardson, Hartmann, Prandtl and Darcy numbers, respectively. The properties of the nanofluid are [4], [5]

effective density, $\rho_{nf} = (1-\chi)\rho_f + \chi\rho_s$, (9)

thermal diffusivity, $\alpha_{nf} = \frac{K_{eff}}{(\rho C_p)_{nf}}$, (10)

heat capacitance, $(\rho C_p)_{nf} = (1-\chi)(\rho C_p)_f + \chi(\rho C_p)_s$ (11)

effective dynamic viscosity, $\mu_{nf} = \frac{\mu_f}{(1-\chi)^{2.5}}$, (12)

thermal expansion coefficient, $(\rho\beta)_{nf} = (1-\chi)\rho_f \beta_f + \chi\rho_s \beta_s$. (13)

Based on Modified Maxwell [15] model, k_{eff} and k_{eq} for spherical nano particles are expressed by

$$\frac{k_{eff}}{k_f} = \frac{(k_{eq} + 2k_f) + 2(k_{eq} - k_f)(1+\omega)^3\chi}{(k_{eq} + 2k_f) - (k_{eq} - k_f)(1+\omega)^3\chi}, \quad (14)$$

$$\frac{k_{eq}}{k_s} = \eta \frac{2(1-\eta) + (1+2\eta)(1+\omega)^3}{-(1-\eta) + (1+2\eta)(1+\omega)^3}, \quad (15)$$

where $\omega = h_{nl}/r_s$. In this analysis, the radius of nano particles (r_s), nano-layer thickness (h_{nl}), and k_{nl} are $3nm$, $2nm$ and $100k_f$. The local (Nu) and the average (Nu_{avg}) Nusselt numbers are calculated by the following formula

That is, $Nu = -\frac{k_{eff}}{k_f}\frac{1}{Ar}\frac{\partial T}{\partial Y}\Big|_{Y=1}$ and $Nu_{avg} = \int_0^{Ar} Nu\, dX$.

3. NUMERICAL TECHNIQUE AND VALIDATION

The equations (5)–(8) are solved by finite volume method (FVM). Coupled pressure and velocity terms are solved by Patankar's [16] SIMPLE algorithm. Discretised equations are solved by TDMA line-by-line method. A grid test is carried out for the different grid sizes at $Ri = 1$, $Da = 10^{-2}$, $Ha = 50$, $\mathrm{Pr} = 6.2$, $Ar = 0.5$, $\gamma = 0^0$, $\varepsilon = 0.4$ and $\chi = 0.06$. Table. 2 shows the result of grid independence test in terms of Nu_{avg} and confirms that the size of 41×81 grid is adequate for the numerical calculations. The precision of the current numerical calculations evaluated with the results Arefmanesh and Mahmoodi [17]. The results are shown in Figure 2, which confirms the accurateness of current numerical simulations.

Table 2: Average Nusselt Number for Grid Independence Test at $Da=10^{-2}$, $Ar=0.5$, $Ha=50$, $\gamma=0^0$, $\Pr=6.2$, $Ri=1$, $\varepsilon=0.4$ and $\chi=0.06$.

Grid Size	11 X 21	21 X 41	41 X 81	81 X 161
Nu_{avg}	0.655356	0.603069	0.602169	0.602275

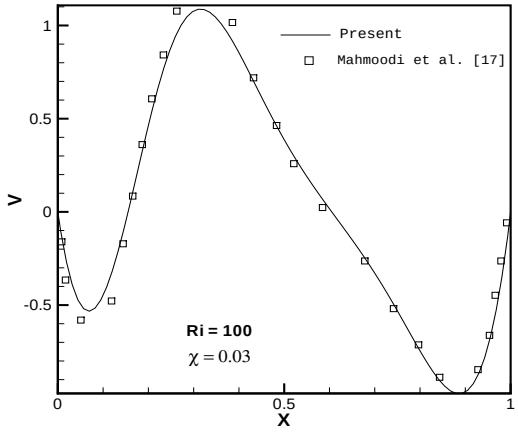

Figure 2: Comparison of the Current Results with the Results of Khanafer and Chamka [17].

4. RESULTS AND DISCUSSIONS

This article aims to discussing numerically the impacts of magnetic field orientations on combined convection of nanofluid in a rectangular porous cavity. The top wall is heated uniformly and it is set to move from left to right. Constant cold temperature wall is fixed at bottom. The vertical sidewalls remain adiabatic. The cavity is filled with nanofluid with $\Pr=6.2$. The porosity is fixed as $\varepsilon=0.4$. The $Ri=Gr/\mathrm{Re}^2$ is chosen as 1throughout the study. The results are illustrated for various values of Ha $(0\le Ha\le 70)$, solid volume fractions $(0\le\chi\le 0.06)$, Da $(0.0001\le Da\le 0.1)$ and the inclination angles of magnetic field $(0^0\le\gamma\le 90^0)$. Moreover, the aspect ratio, Ar is considered as the ratio of length (L) and height (H).

Figure 3 demonstrates the isotherms and streamlines for various values of γ at $Ha=50$ and $Ar=0.5$. When $\gamma=0^0$, the flow inside the enclosure is characterized by a counter clockwise (CCW) circulating cell at the top and a clockwise (CW) circulating cell with two kernels below the top vortex. The temperature contours indicate the heat is transferred by conduction mode. For $\gamma=30^0$, the two kernels of the bottom cell is merged and both the vortices are elongated diagonally. Further tilting the magnetic field to $\gamma=60^0$, the top vortex increases in its sizes and squeezes the bottom vortex. The isotherms near the left sidewall at top part of the enclosure are moved towards the cold wall. When $\gamma=90^0$, the bottom vortex vanishes and the top cell engages the total enclosure. The slope of isotherms is increased so that the rate of heat transfer is improved.

Figure 4 displays the thermal pattern and fluid flow for different inclinations of magnetic field at $Ha=50$ and $Ar=2$. At $\gamma=0^0$, the cavity is filled with a large CCW rotating cell below the small CW rotating cell. The isotherms are almost perpendicular to the vertical wall at lower part and slanted type of isotherms appears at top part of the cavity.

Directions of applied magnetic field differ from horizontal to vertical, the fluid flow field and temperature distribution are affected. The bottom cell vanishes and the top cell engages the full cavity. The distribution of temperature contours is collapsed. Figure 5 displays the heat transfer rate for various γ. The Nu_{avg} enhances with an amplification of γ. The heat transfer rate for horizontal cavity is higher than that of the vertical cavity.

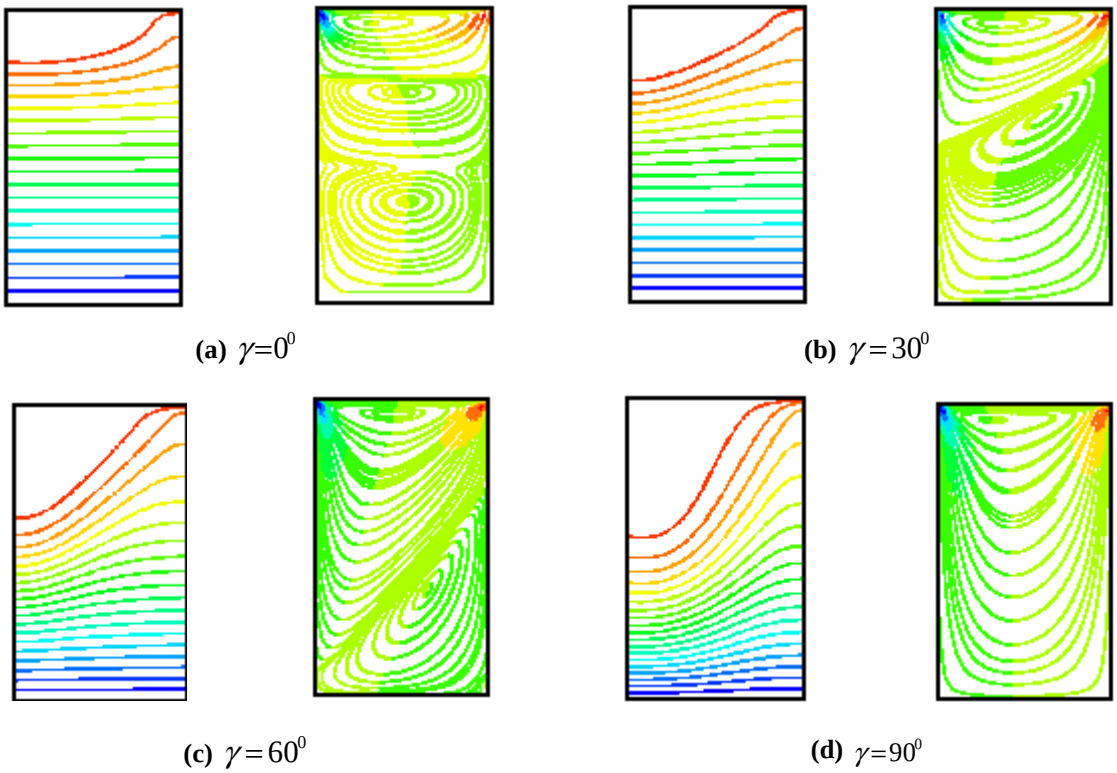

(a) $\gamma=0^0$ **(b)** $\gamma=30^0$

(c) $\gamma=60^0$ **(d)** $\gamma=90^0$

Figure 3: Isotherms and Streamlines for Different γ **at** $Ri=1$, $Ha=50$, $Da=10^{-2}$, $\chi=0.06$ **and** $Ar=0.5$.

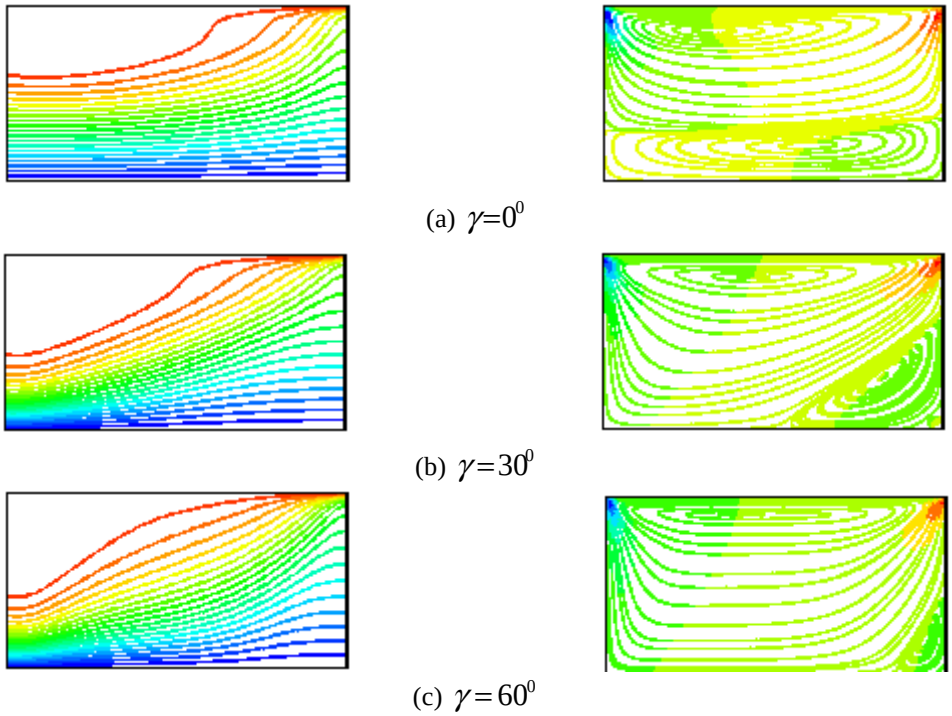

(a) $\gamma=0^0$

(b) $\gamma=30^0$

(c) $\gamma=60^0$

(d) $\gamma=90^0$

Figure 4: Isotherms and Streamlines for Different γ at $Ri=1$, $Da=10^{-2}$, $Ha=50$, $\chi=0.06$ and $Ar=2$.

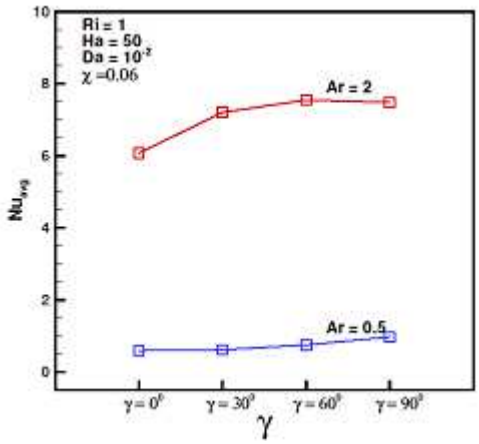

Figure 5: Average Nusselt Numbers for Different Ar and γ with $Ri=1$, $Da=10^{-2}$ and $\chi=0.06$.

Figure 6 demonstrates the results of Ha on streamlines and isotherms at $\gamma=0^0$ and $Ar=0.5$. For $Ha=0$, the enclosure is filled with two cells, one below the other. The corresponding isotherms are distributed horizontally at lower part of the cavity and skewed type of isotherms appears at upper part of the cavity. When $Ha=20$, the flow is categorized by tri-cellular flow structure. The temperature contours are pushed upward. For $Ha=70$, the four cellular flow configurations is formed. The isotherms are straightened and conduction form of heat transfer exists. The isotherms and streamlines for various Ha with $\gamma=0^0$ and $Ar=2$ are depicted in Figure 7. When $Ha=0$, a large CW rotating cell occupies almost the whole cavity with a small eddy appears at the lower left part of the enclosure. The consequent isotherms represent that high temperature gradient at lower left part of the enclosure. On increasing Ha, the small vortex grows bigger and compresses the primary vortex. The temperature contours are pushed upward and extend the entire cavity.

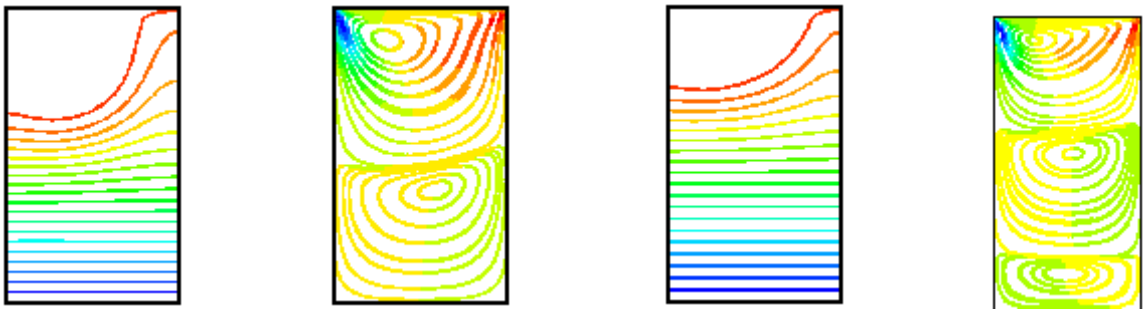

(a) $Ha=0$ (b) $Ha=20$

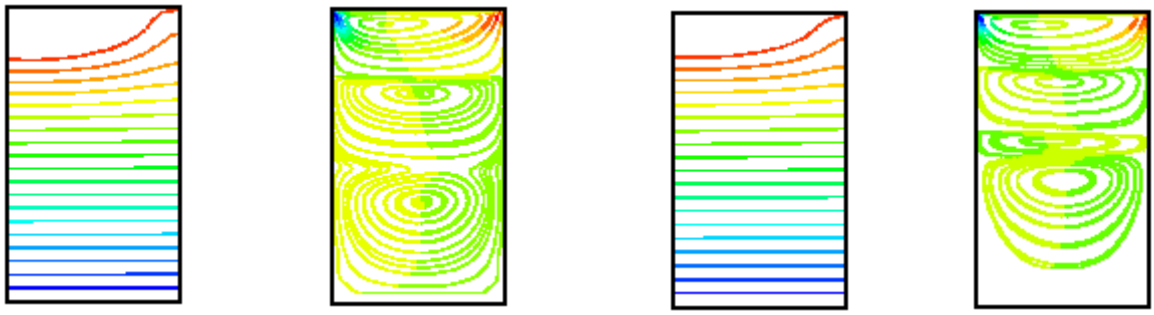

(c) Ha=50 (d) Ha=70

Figure 6: Isotherms and Streamlines for Different Ha at Ri=1, $Da=10^{-2}$, $\gamma=0^0$, $\chi=0.06$ and $Ar=0.5$.

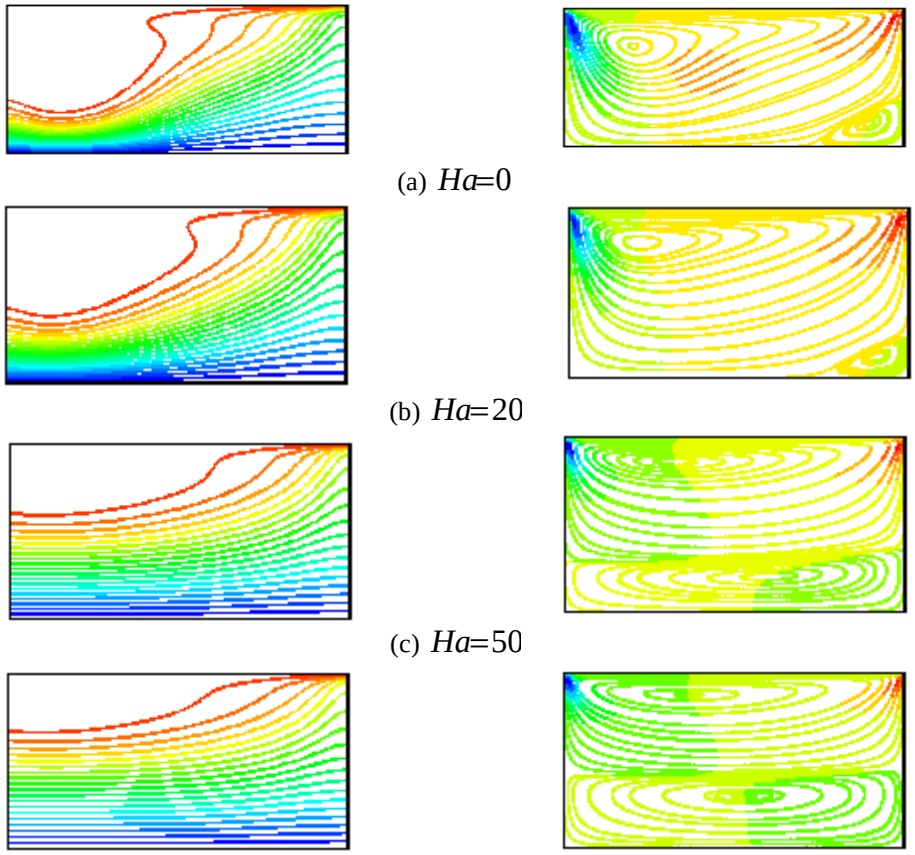

(a) Ha=0

(b) Ha=20

(c) Ha=50

(d) Ha=70

Figure 7: Isotherms and streamlines for different Ha at $Ri=1$, $\gamma=0^0$, $Da=10^{-2}$, $\chi=0.06$ and $Ar=2$.

Figure 8 illustrates the Nu_{avg} for various values of Ha. The heat transfer rate diminishes with the growing of Ha. The effect of magnetic field is high for horizontal cavity than the vertical cavity. The effect of K over χ is plotted in the Figure 9. In this case, Ha is chosen as 50. In the presence of magnetic field, an enhancement in the χ marks in the raise in Nu_{avg} whether K and Ar are considered or not. When $Ar=2$, the higher value of K boosts the heat transfer rate, than the lower value of K.

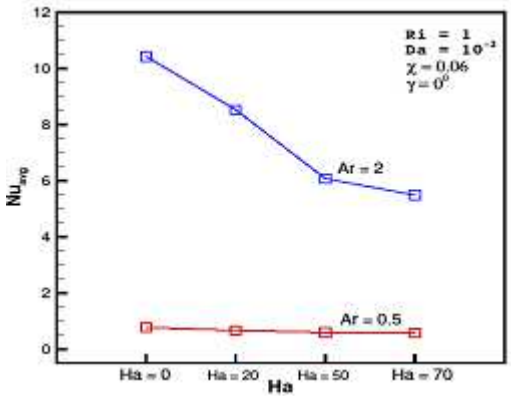

Figure 8: Average Nusselt Numbers for Different Ha **with** $Ri=1$, $Da=10^{-2}$ **and** $\chi=0.06$

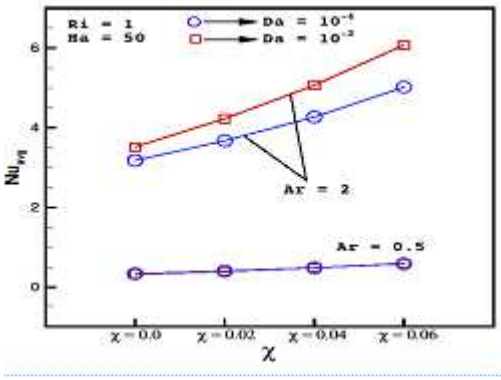

Figure 9: Average Nusselt Numbers for Different Da **and** χ **with** $Ri=1$, $Ha=50$ **and** $\gamma=0^0$.

5. CONCLUSIONS

The consequences of magnetic field with its directions in a rectangular porous cavity filled with nanofluid are examined, numerically. The top wall is heated uniformly and a constant cold temperature is maintained at the bottom wall. The remaining walls are fully insulated. The obtained results are given below:

- The inclination angles of applied magnetic field augment the heat transfer rate.
- Amplification in the Hartmann number and the orientation of applied magnetic field change the fluid flow and heat transfer characteristics.
- By growing Ha, the Nu_{avg} is decreased in the shallow cavity, where as it has no effect in the slender cavity.
- The effect of Darcy number is observed on heat transfer rate only when $Ar = 2$.
- In spite of K and Ar, an enhancement in the χ of nanofluid raises the rate of overall heat transfer in the existence of magnetic field.

REFERENCES

1. *Bourantas. G. C.; Skouras. E. D.; Loukopoulos. V. C.; Burganos. V. N. (2013). Heat Transfer and Natural Convection of Nanofluids in porous Media. Eur. J. Mech.-B/Fluids, 43, 45–56.*

2. *Mittal. N.; Manoj. V.; Kumar. D. S., & Satheesh. A. (2103). Numerical Simulation of Mixed Convection in a Porous Medium Filled with Water/Al_2 O_3 Nanofluid. Heat Transfer—Asian Research, 42(1), 46–59.*
3. *Shekar. B. C.; Kishan, N. (2015) Finite Element Analysis of Natural Convective Heat Transfer in a Porous Square Cavity Filled with Nanofluids in the Presence of Thermal Radiation. In Journal of Physics: Conference Series. 2015, 662, No. 1, 012017). IOP Publishing.*
4. *Kefayati. G. H. R. (2016) Heat Transfer and Entropy Generation of Natural Convection on Non-Newtonian Nanofluids in a Porous Cavity. Powder Technology. 299, 127–149.*
5. *Qashqaei, A., & ASL, R. G. (2015). Numerical Modeling and Simulation of Copper Oxide Nanofluids used in Compact Heat Exchangers. International Journal of Mechanical Engineering, 4 (2), 1, 8.*
6. *Hashemi. H.; Namazian. Z.; Mehryan. S. A. M. (2017) Cu-water Micropolar Nanofluid Natural Convection within a Porous Enclosure with Heat Generation. Journal of Molecular Liquids. 236, 48–60.*
7. *Ghalambaz. M.;, Sabour. M.; Pop. I. (2016) Free Convection in a Square Cavity Filled by a Porous Medium Saturated by a Nanofluid: Viscous Dissipation and Radiation Effects. Engineering Science and Technology, an International Journal.19(3), 1244–1253.*
8. *Astanina. M. S.; Sheremet. M. A.; Oztop. H. F.; Abu-Hamdeh. N. (2018) Mixed Convection of Al2O3-Water Nanofluid in a Lid-Driven Cavity having Two Porous Layers. International Journal of Heat and Mass Transfer. 118, 527–537.*
9. *OwaiD, A. I., Tariq, M., Issa, H., Sabeeh, H., & Ali, M. The Heat Losses Experimentally in the Evacuated Tubes Solar Collector System in Baghdad-Iraq Climate.*
10. *Chamkha. A. J. (2002) Hydromagnetic Combined Convection Flow in a Vertical Lid-Driven Cavity with Internal Heat Generation or Absorption. Numerical Heat Transfer: Part A: Applications. 41(5), 529–546.*
11. *Malleswaran, A.; Sivasankaran. S.; Bhuvaneswari. M. (2013) Effect of heating location and size on MHD Mixed Convection in a Lid-Driven Cavity. International Journal of Numerical Methods for Heat & Fluid Flow. 23(5), 867–884.*
12. *Muthtamilselvan. M.; Doh. D. H. (2014) Magnetic Field Effect on Mixed Convection in a Lid-Driven Square Cavity Filled with Nanofluids. Journal of Mechanical Science and Technology. 28(1), 137–143.*
13. *Elshehabey. H. M.; Ahmed. S. E. (2015) MHD Mixed Convection in a Lid-Driven Cavity Filled by a Nanofluid with Sinusoidal Temperature Distribution on the both Vertical Walls using Buongiorno's Nanofluid Model. International Journal of Heat and Mass Transfer. 88, 181–202.*
14. *Hussain. S.; Mehmood. K.; Sagheer. M. (2016) MHD mixed convection and entropy generation of water–alumina nanofluid flow in a double lid driven cavity with discrete heating. Journal of Magnetism and Magnetic Materials. 419, 140–155.*
15. *Thakur, G., & Singh, G. (2017). Experimental Investigation of Heat Transfer Characteristics in Al2O3-Water Based Nanofluids Operated Shell and Tube Heat Exchanger with Air Bubble Injection. International Journal of Mechanical and Production, 7, 263–273.*
16. *Wang. Q. W.; Zeng. M.; Huang. Z. P.; Wang. G.; Ozoe. H. (2007) Numerical Investigation of Natural Convection in an Inclined Enclosure Filled with Porous Medium under Magnetic Field. International Journal of Heat and Mass Transfer. 50(17–18), 3684–3689.*
17. *Grosan. T.; Revnic. C.; Pop. I.; Ingham. D B. (2009). Magnetic Field and Internal Heat Generation Effects on the Free Convection in a Rectangular Cavity Filled with a Porous Medium. International Journal of Heat and Mass Transfer, 52(5–6), 1525–1533.*

18. *Maxwell. C. A (1904). Treatise on Electricity and Magnetism. Second ed, Oxford University, Press, Cambridge 435–441.*
19. *Bodade, P. R., Jogi, N., Gorde, M., Paropte, R., & Waghchore, R. Use of Internal Threads of Different Pitches to Enhance Heat Transfer in A Circular Channel.*
20. *Patankar. S. (1980). Numerical Heat Transfer and Fluid Flow. CRC Press.*
21. *Arefmanesh. A.; Mahmoodi M. (2011). Effects of Uncertainties of Viscosity Models for Al2O3–Water Nanofluid on Mixed Convection Numerical Simulations. International Journal of Thermal Science. 50(9), 1706–1719.*

AUTHOR'S PROFILE

S.Muthukumar received his M.Sc. degree in Mathematics from Periyar University, India, in 2005 and M.Phil, degree in Mathematics from Bharathidasan University, India, in 2006. Currently, he is doing Ph.D. in Periyar University. His research interest is convective heat and mass transfer in enclosures. He has published two research papers in the reputed journals. Presently he is working as Assistant Professor, Department of Mathematics at K.S.Rangasamy College of Technology, Namakkal. He has over 13 years of teaching experience. He is a life member of ISTE.

Dr. Eswari Prem has been working as an Assistant Professor in PG and Research Department of Mathematics, Govt. Arts College for Men, Krishnagiri, India since 2007. She obtained her M.Sc. and M.Phil, from Madras University, India in 1989 and 1990 and Ph.D from Periyar University, India in 2011. She is having a total teaching experience of 24+ years. She has guided around 16 M.Phil, projects till now. Her research interests include computational fluid dynamics, intuitionistic fuzzy algebra and stochastic models. She has published around 10 research papers international journals.

Dr.S. Sureshkumar, received his M.Sc., degree in Mathematics from Bharathiar University, India, in 2010, M.Phil, degree in Mathematics from Bharathidasan University, India, in 2011, and his Ph.D. degree in Mathematics from Bharathiar University, in 2017. He is serving the Department of Mathematics, Kongu Engineering College Erode, India, as an Assistant Professor since 2017. He is having a total teaching experience of 5 years. His research interest is convection in cavity and he has published 8 research papers in peer reviewed journals.